Published in final edited form as:
Alcohol Clin Exp Res. 2014 September ; 38(9): 2414–2426. doi:10.1111/acer.12525.

Acute Alcohol Intoxication-Induced Microvascular Leakage

Travis M. Doggett, B.S.[1] and **Jerome W. Breslin, Ph.D.**[2]

[1]Department of Physiology, School of Medicine, Louisiana State University Health Sciences Center, New Orleans, LA

[2]Department of Molecular Pharmacology and Physiology, Morsani College of Medicine, University of South Florida, Tampa, FL

Abstract

Background—Alcohol intoxication can increase inflammation and worsen injury, yet the mechanisms involved are not clear. We investigated whether acute alcohol intoxication elevates microvascular permeability, and investigated potential signaling mechanisms in endothelial cells that may be involved.

Methods—Conscious rats received a 2.5 g/kg alcohol bolus via gastric catheters to produce acute intoxication. Microvascular leakage of intravenously administered FITC-albumin from the mesenteric microcirculation was assessed by intravital microscopy. Endothelial-specific mechanisms were studied using cultured endothelial cell monolayers. Transendothelial electrical resistance (TER) served as an index of barrier function, before and after treatment with alcohol or its metabolite acetaldehyde. Pharmacologic agents were used to test the roles of alcohol metabolism, oxidative stress, p38 mitogen-activated protein (MAP) kinase, myosin light chain kinase (MLCK), rho kinase (ROCK), and exchange protein activated by cAMP (Epac). VE-cadherin localization was investigated to assess junctional integrity. Rac1 and RhoA activation were assessed by ELISA assays.

Results—Alcohol significantly increased FITC-albumin extravasation from the mesenteric microcirculation. Alcohol also significantly decreased TER and disrupted VE-cadherin organization at junctions. Acetaldehyde significantly decreased TER, but inhibition of ADH or application of a superoxide dismutase mimetic failed to prevent alcohol-induced decreases in TER. Inhibition of p38 MAP kinase, but not MLCK or ROCK, significantly attenuated the alcohol-induced barrier dysfunction. Alcohol rapidly decreased GTP-bound Rac1 but not RhoA during the drop in TER. Activation of Epac increased TER, but did not prevent alcohol from decreasing TER. However, activation of Epac after initiation of alcohol-induced barrier dysfunction quickly resolved TER to baseline levels.

Conclusions—Our results suggest that alcohol intoxication increases microvascular permeability to plasma proteins. The data also suggest the endothelial-specific mechanism involves the p38 MAP kinase, Rac1, and reorganization of VE-cadherin at junctions. Lastly, activation of Epac can quickly resolve alcohol-induced endothelial barrier dysfunction.

Address correspondence to: Jerome W. Breslin, PhD Department of Molecular Pharmacology and Physiology University of South Florida 12901 Bruce B. Downs Blvd. MDC8 Tampa, FL 33612 Tel: 813-974-7631 Fax: 813-974-3079 jbreslin@health.usf.edu.

Keywords

Ethanol; Ethanol Intoxication; Binge Drinking; Microvascular Permeability; Endothelium

INTRODUCTION

Acute alcohol intoxication accounts for the majority of alcohol-related disorders encountered in emergency rooms (Howard et al., 2011). Intoxicated trauma patients present a complex, altered physiologic state, often with increased initial injury severity (Jurkovich et al., 1992, Vonghia et al., 2008). One particularly problematic outcome of acute alcohol intoxication is aggravated hemodynamic instability following hemorrhage (Shih et al., 2003). Intoxicated trauma patients are frequently hypotensive, requiring significantly greater volumes of resuscitative fluids and blood products compared to non-intoxicated patients (Bilello et al., 2011, Fabbri et al., 2001, Shih et al., 2003). Several studies have postulated that an impaired baroreceptor reflex or associated neural, endocrine, and metabolic mechanisms that control vascular tone may be responsible (Greiffenstein et al., 2007, Mathis et al., 2006, Molina et al., 2004, Phelan et al., 2002). However, more recent studies have shown that sympathetic control of blood pressure and acetylcholine-induced vasodilation are not impaired by alcohol intoxication (Mathis and Molina, 2009, Molina et al., 2009). Such findings led us to investigate whether alcohol impacts vascular mechanisms other than those that focus on vascular tone, such as microvascular permeability.

Inflammatory stimuli typically increase microvascular permeability to macromolecules in postcapillary venules (Duran et al., 2008). Endothelial cells play an active role in the control of microvascular permeability, and several intracellular signaling mechanisms coordinate to reduce endothelial barrier integrity. These include increased activity of PKCβ, IP_3/Ca^{2+}/calmodulin-mediated activation of myosin light chain kinase (MLCK), activation of the RhoA/rho kinase (ROCK) pathway, inactivation of Rac1/Cdc42, eNOS/cGMP/PKG signaling, MAPK activation, cytoskeletal changes, and alteration of junctional and focal adhesions (Duran et al., 2010, Yuan, 2000). Previous studies have shown that alcohol can increase the permeability of cultured brain endothelial cell monolayers. (Haorah et al., 2005a, Haorah et al., 2007). These studies identified that alcohol activates some of the aforementioned signaling pathways, such release of Ca^{2+} from intracellular stores, MLCK-mediated cytoskeletal reorganization and disruption of the tight junction proteins ZO-1, claudin, and occludin (Haorah et al., 2005a, Haorah et al., 2007). In addition, the products of alcohol metabolism, namely the metabolite acetaldehyde and increased oxidative stress, both promoted increased permeability of brain endothelial cell monolayers (Haorah et al., 2005b).

One question not previously addressed is whether alcohol intoxication may increase microvascular permeability in non-neural tissues. Ingested alcohol initially enters the bloodstream from the digestive tract, a very susceptible site of injury in alcohol-intoxicated trauma victims. With this in mind we tested the hypothesis that alcohol intoxication increases microvascular leakage in the mesenteric microcirculation, using a rat model that reflects a binge-drinking episode. To explore potential subcellular mechanisms within endothelial cells, we utilized cultured endothelial cell models for functional and biochemical

analyses. The mechanisms focused upon within this study included alcohol metabolism, oxidative stress, p38 MAPK signaling, MLCK, the small GTPase RhoA and its downstream effector ROCK, the small GTPase Rac1, and the barrier enhancing signaling molecule known as the exchange protein activated by cAMP (Epac).

MATERIALS AND METHODS

Animals

All animal protocols were performed in strict accordance with the U.S. Animal Welfare Act, U.S. Public Health Service Policy on the Humane Care and Use of Laboratory Animals, and the *Guide for the Care and Use of Laboratory Animals*. All animal experiments were performed after approval from the Louisiana State University Health Sciences Center – New Orleans Institutional Animal Care and Use Committee (Permit Number: 2816) and the University of South Florida Institutional Animal Care and Use Committee (Permit Number 4364R). All surgery was performed after the rats were anesthetized, and all efforts were made to minimize suffering. Sprague-Dawley rats (Charles River, Wilmington, MA) (325-350 g) were provided a standard diet (Purina Rat Chow, Ralston Purina, St. Louis, MO) and water ad libitum and were housed in a 12 h light/12 h dark cycle for a one-week acclimation period prior to surgery.

Surgical Preparation and Alcohol Administration

Alcohol was administered to conscious, unrestrained rats using a previously established model simulating a binge-drinking episode, which produces blood alcohol concentrations in the 200-300 mg/dL range 30 minutes after administration (Souza-Smith et al., 2010, Souza-Smith et al., 2013). The surgical preparation for the model has been previously described in detail (Molina et al., 2009, Molina et al., 2004). Briefly, rats were anesthetized with ketamine and xylazine (90 and 9 mg/kg, respectively), and sterile catheters were implanted in the left common carotid artery and the right external jugular vein. An additional intragastric catheter was also implanted, secured with a purse-string suture. All catheters were flushed with 0.9% sterile Sodium Chloride USP (Baxter, Deerfield, IL), thermally sealed, and routed subcutaneously using a trocar to the dorsal nape of the neck. Catheters were secured to the closed incision with suture, coiled, and wrapped with masking tape to prevent animal interference. Carotid catheters were used for blood pressure monitoring and blood sample withdrawal. Jugular catheters were used for administration of fluorescent tracer for intravital microscopy. Gastric catheters were used for alcohol administration. After surgery, animals were allowed 2-3 days of recovery in the same conditions as the acclimation period before experiments.

Conscious, unrestrained rats received an intragastric bolus of alcohol (30% ethyl alcohol by volume) at 2.5 g/kg via the gastric catheter. A time-matched control group received isovolumic administration of vehicle (water). After alcohol or vehicle administration, rats were allowed to roam in their cages for 30 minutes before undergoing anesthesia (ketamine/xylazine 90 mg/kg and 9 mg/kg, respectively) and surgical prep for intravital microscopy.

In Vivo Assessment of Microvascular Leakage

Microvascular leakage was assessed by intravital microscopy of the mesenteric microcirculation as previously described (Breslin et al., 2008, Breslin et al., 2007, Reynoso et al., 2007). Briefly, rats were anesthetized, ventral abdominal fur was shaved, and the skin cleaned using 4% Chlorhexidine gluconate solution (CareFusion, Leawood, KS), 100% ethanol, and 7.5 % Povidone-iodine (Purdue Products L.P., Stamford, CT). A midline laparotomy was performed and the small intestine was exteriorized and splayed over an optical stage. The mesentery was superfused with 37 °C albumin-based physiological salt solution (APSS; NaCl, 120 mM; KCl, 4.7 mM; $CaCl_2 \cdot 2H_2O$, 2 mM; $MgSO_4 \cdot 7H_2O$, 1.2 mM; NaH_2PO_4, 1.2 mM; Na pyruvate, 2 mM; glucose, 5 mM; EDTA, 0.02 mM; MOPS, 3 mM, purified BSA 1 g/100ml, pH 7.4). Body temperature was maintained by a thermal plate and monitored by rectal thermometer. Blood pressure was monitored from the carotid catheter with a pressure transducer and computer (AD Instruments, Colorado Springs, CO). Fluorescein isothiocyanate (FITC) conjugated albumin (FITC-albumin) dissolved in Ringer's lactate solution was administered to the jugular vein as a bolus (1 mg/10 kg over 1-2 minutes) followed by continuous infusion (0.15 mg/kg/min). Epifluorescent images of the mesenteric microcirculation were obtained at 10-min intervals for 1 h with a Nikon Eclipse E600 fluorescent microscope using a 10x objective (Nikon Instruments Inc., Natick, MA) at 488 nm excitation. Images were captured with a ThorLabs USB 2.0 Digital Camera (ThorLabs, Newton, NJ) controlled with Micromanager software (Edelstein et al., 2010). FITC-albumin extravasation was quantified by measuring the integrated optical intensity (IOI) of extravascular regions near postcapillary venules (Breslin et al., 2008, Breslin et al., 2007, Reynoso et al., 2007, Duran et al., 2008). The maximal change in IOI from the 0-min time point during the 60-min time course was used to compare FITC-albumin extravasation between groups. Arteriole diameters in the same images were also measured to test for potential differences between groups.

Endothelial Cell Culture

Human umbilical vein endothelial cells (HUVEC) and human cardiac microvascular endothelial cells (HMVEC-c) were obtained from Lonza (Allendale, NJ) and grown in endothelial growth medium (EGM2MV; Lonza) on 1.5% porcine gelatin matrix (Sigma-Aldrich, St. Louis, MO) in a 37°C, 5% CO_2 incubator. HUVEC were used at passages 1-4 and HMVEC-c at passages 4-8.

Determination of Endothelial Barrier Function

Barrier function was determined by assessing transendothelial electrical resistance (TER) of confluent HUVEC or HMVEC-c monolayers, using an Electric Cell/Substrate Impedance Sensing (ECIS) ZΘ system (Applied Biophysics, Troy, NY). Cells were subcultured onto gelatin-coated gold-plated 8W1E ECIS electrode arrays (1.5-1.75 × 10^5 cells/well) in EGM2MV medium. The arrays were attached to the ECIS station in a 37°C, 5% CO_2 incubator for overnight monitoring as the cells formed a confluent monolayer. Prior to experiments, the medium was changed to endothelial basal medium (EBM; Lonza) and the cells were allowed to reestablish a steady baseline TER within a range of 8,000-12,000 Ω. Both HUVEC and HMVEC-c achieved baseline TER within this range. To test whether

alcohol produced a concentration-related response, the cells were treated with 20, 50, or 100 mM ethyl alcohol. The ability of acetaldehyde (Sigma-Aldrich) to alter TER was also tested at concentrations of 5, 10, and 20 mM. The role of alcohol metabolism was tested with 1 mM 4-methylpyrazole (4-MP; Axxora, Farmingdale, NY) (Haorah et al., 2005b). Oxidative stress was also investigated with the superoxide dismutase (SOD) mimetic MnTMPyP (4 or 40 μM; Merck-Millipore, Billerica, MA) and the peroxide scavenger EUK-134 (25 or 50 μM; Cayman Chemical, Ann Arbor, MI) prior to addition of alcohol (Mountain et al., 2007). The roles of MLCK, ROCK, p38 MAPK were tested with 1 μM ML-7, 5 μM Y-27632, and 6, 10, and 20 μM SB203580, respectively (Merck-Mililpore) (Borbiev et al., 2004, Garcia et al., 2002, Lal et al., 2001, Kurtz et al., 2014). The role of Epac was tested using the selective Epac activator 8-CPT-2'-O-Me-cAMP (8-CPT; 100 μM, Merck-Millipore) (Adamson et al., 2008, Birukova et al., 2010, Baumer et al., 2008).

Rac1 Activation Assay

The pool GTP-bound RhoA or Rac1 was measured using the RhoA and Rac1 G-LISA activation assay (Cytoskeleton, Inc., Denver, CO, USA). HUVEC were grown in 10 cm culture dishes to confluence. Medium was changed to EBM for 6 h prior to experiments to alleviate potential confounding effects of serum. The cells were treated with 100 mM alcohol for 1, 5, 10, 30, or 60 min before a wash with ice-cold PBS, and addition of 250 μL ice-cold lysis buffer containing protease inhibitors. The cells were quickly scraped and harvested, clarified by centrifugation at 14000 × g, 4 °C for 2 min, and the supernatants snap-frozen in liquid nitrogen. Protein concentrations were determined with the Precision Red™ Advanced Protein Assay (Cytoskeleton, Inc.) using an Infinite 200 PRO Nanoquant system (Tecan, Männedorf, Switzerland). Protein concentrations ranged from 1.75-2.00 mg/mL and were equalized for the assay. GTP-bound levels of RhoA or Rac1 were determined in 96-well RhoA-GTP or Rac1-GTP binding plates, using a lysis buffer blank negative control and 80 pg/ml recombinant GTP-bound RhoA or Rac1 positive controls. Luminescence was determined with the Infinite 200 PRO Nanoquant system.

Immunofluorescence labeling

Immunofluorescence labeling of VE-cadherin in cultured endothelial cells treated with alcohol was assessed to determine the impact of alcohol on intercellular junctions. Confluent cells grown on gelatin-coated glass coverslips were first incubated 24 hours in EBM to alleviate potential confounding factors caused by serum. After treatment with alcohol or other agents (as indicated in the results), cells were fixed in 4% paraformaldehyde and permeabilized in 0.1% Triton-X100 buffer. The cells were labeled with a primary antibody to VE-cadherin (C-19, Santa Cruz Biotechnologies, Santa Cruz, CA) and an Alexafluor 488 conjugated secondary antibody (Life Technologies, Carlsbad, CA). The coverslips were mounted onto glass microscope slides using Vectashield with DAPI (Vector Laboratories, Burlingame, CA). Images were collected with a Nikon TE-2000U microscope system (Nikon Instruments).

Transfection and Time-Lapse Imaging of Endothelial Cells

The Nucleofector II system (Lonza) was used to transfect HUVEC with plasmids encoding VE-cadherin-GFP (Delanoe-Ayari et al., 2004a, Delanoe-Ayari et al., 2004b) generously

provided by Dr. Daniel Riveline (Institut de Science et d'Ingénierie Supramoléculaires, Université de Strasbourg, France). For each transfection, 5×10^5 cells were combined with 2 μg plasmid DNA. The cells were subcultured onto gelatin-coated 35-mm #1 glass culture dishes (MatTek, Inc. Ashland, MA) and used 1-2 days after plating for imaging studies.

The glass-bottom culture dishes containing transfected cells were placed onto a heated stage connected to a temperature controller (Warner Instruments DH-35il & TC-344b, Hamden, CT). An open perfusion chamber insert featuring an in-flow port and an outflow vacuum port was placed into the culture dish (Warner Instruments RC-37F). The cells were superfused with APSS at 37 °C, gravity fed from a 60 cc syringe reservoir, controlled by a flow regulator, and warmed to 37 °C by an inline heater (Warner Instruments SH-27B). Time-lapse images were obtained with a Nikon Eclipse TE-2000U system equipped with a Sutter Instruments Lambda LS 300 W xenon lamp, Lambda 10-3 excitation filter wheel with S492, S572, and D350 filters, and SmartShutter (Sutter Instruments, Novato, CA). Using Nikon Elements AR software, images were captured every minute for a 30-minute baseline and after addition of 100 mM alcohol to the bath and reservoir (30 additional minutes).

Data Analysis

For time course data, tracings of the means are shown. Summarized data are presented as means ± SE, and were evaluated by ANOVA followed by Tukey's test when appropriate to compare all groups. Significance was accepted at $P<0.05$.

RESULTS

Alcohol caused a noticeable extravasation of FITC-albumin from the mesenteric microcirculation, compared to controls (Fig. 1*A*, *B*). The mean maximal change in IOI in the extravascular space adjacent to postcapillary venules was significantly higher in the alcohol-treated rats compared to controls (Fig. 1*C*). Mean arteriolar diameter was also assessed to determine whether changes in blood flow may contribute to the overall response. There was no significant difference in mean arteriolar diameter between the alcohol and control groups, supporting the notion that increased permeability of the venular endothelium primarily contributed to the observed macromolecule leakage (Fig. 1*D*). The direct impact of alcohol on endothelial barrier function was also tested, using cultured HUVEC or HMVEC-c monolayers. Alcohol caused a decrease in TER, an index of barrier integrity, of HUVEC and HMVEC-c. Alcohol at 50 or 100 mM significantly decreased TER, compared to control (Fig. 2).

Previous studies modeling alcohol-induced blood brain barrier dysfunction showed disruption of tight junction proteins (Haorah et al., 2005a, Haorah et al., 2007, Haorah et al., 2005b). We evaluated the organization of a different, endothelial-specific junctional protein, VE-cadherin, due to its critical role in peripheral microvascular barrier function (Corada et al., 1999). Control HUVEC displayed continuous VE-cadherin labeling at cell-cell junctions, which became noticeably fragmented in alcohol-treated cells within 5 minutes (Fig. 3*A*). This finding was confirmed using time-lapse microscopic imaging of live HUVEC expressing VE-cadherin-GFP (Fig. 3*B*). These data indicate that the alcohol-

induced decreases in TER occur concurrently with structural changes in the paracellular junctions between endothelial cells.

To gain insight into the mechanism of action we examined the potential role of alcohol metabolism by ADH to acetaldehyde, which was previously shown to contribute to disruption of brain microvascular endothelial cell (BMVEC) barrier integrity (Haorah et al., 2005b). In the current study, acetaldehyde at concentrations of 10 and 20 mM significantly decreased TER of HUVEC (Fig. 4). Notably, 10 mM acetaldehyde elicited a decrease in TER that was equivalent in magnitude to that caused by 100 mM alcohol (Fig. 4), suggesting a potency approximately 10 times higher than alcohol. However, inhibition of ADH by pretreatment with 1 mM 4-MP for 30 min did not prevent alcohol-induced decreases in TER (Fig. 5). This result suggests that cultured peripheral endothelial cells may not require metabolism of alcohol in order for alcohol-induced barrier dysfunction to occur.

Formation of reactive oxygen species (ROS) was also previously reported to contribute to alcohol-induced blood brain barrier dysfunction (Haorah et al., 2011). We tested the role of ROS by pretreating endothelial monolayers with the SOD mimetic MnTMPyP before addition of alcohol. Pretreatment of HUVEC with 4 or 40 μM MnTMPyP for 30 min did not block the alcohol-induced endothelial barrier function (Fig. 6*A, B*). In addition, we employed the ROS scavenger EUK-134 (25 or 50 μM) which also failed to block the alcohol-induced decrease in TER (Fig. 6*C, D*), suggesting that oxidative stress may not play a significant role in this model.

We also tested the role of p38 MAPK, which can be activated by cell stress and has been shown to contribute to inflammation and elevated endothelial permeability (Garcia et al., 2002, Kevil et al., 2001, Lal et al., 2001). Pretreatment for 30 min with SB203580 (6-20 μM) did not impact baseline TER, however did significantly attenuate the alcohol-induced decrease in TER (Fig. 7). SB203580 pretreatment also preserved VE-cadherin junctional structures in the presence of alcohol (Fig. 8). Combined, these data suggest that p38 MAP kinase contributes to the alcohol-induced endothelial barrier dysfunction.

MLCK-mediated phosphorylation of MLC has also been shown to contribute to alcohol-induced disruption of BMVEC monolayers (Haorah et al., 2005a, Haorah et al., 2007), and has been implicated in microvascular hyperpermeability in response to a variety of other agonists (Duran et al., 2008, Mehta and Malik, 2006, Yuan, 2000). Pretreatment of HUVEC monolayers with the MLCK inhibitor ML-7 (1 μM) did not inhibit the ability of alcohol to decrease TER (Fig. 9*A*). This led us to examine alternative signals that influence the actin cytoskeleton, such as the small GTPases RhoA and Rac1 (Spindler et al., 2010, Waschke et al., 2004, Waschke et al., 2006). Alcohol did not affect RhoA-GTP levels at the early time points corresponding to the alcohol-induced decrease in TER, but did significantly reduce RhoA-GTP at 60 min (Fig. 9*B*), during the period of recovery of TER to baseline (Fig 2). Likewise, inhibition of RhoA's downstream effector, ROCK, did not attenuate alcohol-induced decreases in TER (Fig. 9*C*). In contrast, alcohol significantly decreased Rac1-GTP levels at the 1, 5, 10, 30, and 60 min time points, and elevated Rac1-GTP at 90 min., before returning to baseline levels by 120 min after alcohol addition (Fig 9*D*).

The temporal correlation between Rac1-GTP levels and the initial decrease in TER caused by alcohol led us to investigate the Epac/Rap1 pathway, which lies upstream of Rac1 and has been shown to enhance endothelial barrier integrity by activating Rac1 (Birukova et al., 2008, Birukova et al., 2010). HUVEC were pretreated with the specific Epac activator 8-CPT (100 μM), which increased TER for the entire 30 minute pretreatment prior to addition of alcohol (Fig. 10*A*, *B*; Fig. S1). However, 8-CPT did not prevent a decrease in TER when alcohol was added. While the alcohol-induced decrease in TER in cells pretreated with 8-CPT did not reach the same nadir as cells that did not receive 8-CPT, the magnitude of the decrease in TER between these two groups, measured from the time point when alcohol was added, was not significantly different (Fig. 10*C*).

We also tested whether adding 8-CPT post-alcohol treatment may reverse the alcohol-induced decrease in TER. Treatment with 50 or 100 μM 8-CPT at 5 or 10 min after the addition of alcohol caused TER to rapidly rise, establishing a new steady-state TER higher than the initial baseline (Fig. 11*A*, *B*; Fig. S2). The time to return to the initial baseline TER level was significantly reduced after treatment with 8-CPT compared to the vehicle controls (Fig. 11*C*). We next examined changes in VE-cadherin organization in cultured HUVEC that were treated with 100 μM 8-CPT starting 5 min after alcohol was added (Fig. 12*A*). Vehicle-treated controls at both time points displayed the expected disorganized and fragmented VE-cadherin labeling along with paracellular gap formation (Fig. 12*B*, *C*). However, the 8-CPT-treated groups displayed restored VE-cadherin organization with a more continuous, junctional organization with no paracellular gaps (Fig. 12 *D*, *E*). These data suggest that selective activation of the Epac/Rap1 pathway can reverse alcohol-induced endothelial barrier dysfunction.

DISCUSSION

In the current study, we present the first direct evidence that acute alcohol intoxication increases leakage of plasma proteins from the mesenteric microcirculation *in vivo*. We also demonstrate that alcohol can cause significantly reduced barrier function of *in vitro* cultured endothelial cells. These functional changes are accompanied by disruption of VE-cadherin at intercellular junctions, a hallmark of endothelial hyperpermeability. The alcohol metabolite acetaldehyde also disrupts the endothelial barrier, but endothelial cells do not appear to be a significant source of acetaldehyde, as inhibition of ADH fails to block alcohol-induced barrier dysfunction of cultured endothelial monolayers. Likewise, blockade of oxidative stress, which would be expected as a byproduct of alcohol metabolism, also does not inhibit alcohol-induced disruption of endothelial barrier integrity. In contrast, inhibition of the p38 MAP kinase attenuates alcohol-induced barrier dysfunction. Also, alcohol causes a significant decrease in Rac1-GTP that typically promotes barrier integrity, while MLCK and RhoA/ROCK did not appear to play a contributing role. Activation of the Epac/Rap1 pathway, which is upstream of Rac1, enhances endothelial barrier function. This enhancement does not inhibit alcohol from decreasing endothelial barrier integrity, but does prevent reaching a level of hyperpermeability that alcohol produces in the absence of Epac activation. In addition, activation of Epac after alcohol treatment causes rapid resolution of barrier integrity, indicating the ability of this pathway to override the signals activated by

alcohol. Overall, these results suggest that alcohol increases microvascular permeability, and that the p38 MAPK and Rac1 are involved in the mechanism of action.

Very few studies have assessed how alcohol impacts microvascular barrier integrity. Previous studies by Haorah, Persidsky, and their colleagues have demonstrated alcohol-induced barrier dysfunction with an *in vitro* model of the BBB endothelium (Haorah et al., 2011, Haorah et al., 2005a, Haorah et al., 2007, Haorah et al., 2005b). In the current study, we observed that alcohol causes a significant and rapid decrease in TER at concentrations of 50 and 100 mM in both HUVEC and HMVEC-c monolayers. This is consistent with the previous studies, in which 50 mM alcohol caused a significant decrease in BMVEC TER (Haorah et al., 2005b). Unlike previous studies, we also evaluated whether alcohol impacts microvascular leakage *in vivo.* To our knowledge, our study is the first to demonstrate that acute alcohol intoxication increases microvascular leakage in the mesenteric microcirculation.

Concomitant with our observation that alcohol disrupts normal barrier integrity of cultured endothelial cells, we present evidence that alcohol disorganizes the normal junctional conformation of VE-cadherin, and essential component of the endothelial barrier *in vivo* (Corada et al., 1999, Lampugnani et al., 1995, Mehta and Malik, 2006). Our findings are concordant with numerous studies showing that reorganization of VE-cadherin at endothelial cell-cell junctions occurs during elevated microvascular permeability (Duran et al., 2008, Mehta and Malik, 2006, Yuan, 2000) and support the previous observation that alcohol disrupts the tight junctional proteins ZO-1, claudin, and occludin in BMVEC (Haorah et al., 2005a). Taken together, these data suggest that changes in paracellular transport of fluids and solutes are involved in alcohol-induced increases in permeability.

We also investigated the role of metabolism of alcohol into acetaldehyde and ROS, which is mediated by two enzymes, ADH and CYP2E1 (Haorah et al., 2005b). Both are present in BMVEC and their activities are increased by alcohol (Haorah et al., 2005b). We observed that acetaldehyde disrupts HUVEC barrier integrity with potency approximately ten times higher than alcohol, similar to previous observations with BMVEC (Haorah et al., 2005a, Haorah et al., 2007). However, we also found that inhibition of ADH and CYP2E1 with 4-MP did not prevent alcohol-induced decreases in TER. In addition, the SOD mimetic MnTMPyP, previously shown to block superoxide-induced endothelial hyperpermeability (Zhang et al., 2005), did not prevent alcohol-induced endothelial barrier dysfunction. These observations were in contrast to the studies using BMVEC, in which pretreatment with 4-MP prevented alcohol-induced decrease in TER and a role for ROS was implicated (Haorah et al., 2011, Haorah et al., 2005b). The differences between the current study and the previous investigations with BMVEC may reflect a relatively low expression of the alcohol metabolizing enzymes in HUVEC. In our study, the inability of 4-MP or MnTMPyP to prevent barrier dysfunction implies that generation of acetaldehyde or reactive oxygen species was probably minimal. These findings do not discount a role for acetaldehyde and ROS *in vivo* because these would be expected to appear in the plasma due to alcohol metabolism in the liver. This topc represents a future area of study, in which the rates of alcohol metabolite formation, alcohol clearance, and the relative impacts on the microvascular barrier can be concurrently quantified.

Specific binding sites for alcohol on proteins that change function are beginning to emerge. However, study of this phenomenon is still in a nascent stage, and much more about this topic likely remains unknown than known (Howard et al., 2011). Thus, to identify signaling mechanisms that may be involved in alcohol-induced endothelial hyperpermeability, we investigated molecular mediators known to increase permeability in response to inflammatory stimuli. One signaling protein we identified in the current study is the p38 MAP kinase. Interestingly, one previous study showed that acetaldehyde increases phosphorylation of p38 MAP kinase on its regulatory domain, facilitating activation (Li et al., 2004). This enzyme seems to be of general importance for increases in endothelial permeability, as its role has been identified in hyperpermeability responses to several different stimuli (Borbiev et al., 2004, Duran et al., 2008, Garcia et al., 2002, Goldberg et al., 2002, Kiemer et al., 2002).

We expected that MLCK would also mediate the alcohol-induced disruption of the endothelial barrier based on the BMVEC studies (Haorah et al., 2005a, Haorah et al., 2007), however inhibition of MLCK had no effect in the current study. We investigated RhoA/ROCK and Rac1 as alternatives. While RhoA/ROCK did not appear to have a significant role, Rac1-GTP levels decreased rapidly at the same time alcohol decreased TER. Rac1 has a well-described role in promoting endothelial barrier integrity (Adamson et al., 2008, Birukova et al., 2010, Spindler et al., 2010, Waschke et al., 2004), by enhancing cortical actin, focal adhesion, and junctional stability (Adamson et al., 2012, Birukova et al., 2008, Liu et al., 2002). Our current data have similarities with another study in which inhibition of Rac1 with bacterial *Clostridium sordellii* toxin increased permeability in isolated rat microvessels and in cultured endothelial cells, which was attributed to reduction of F-actin content and VE-cadherin adhesion (Waschke et al., 2004).

We also demonstrate that selective activation of Epac can enhance endothelial barrier function and can rapidly resolve alcohol-induced disruption of barrier integrity. Epac activates Rap1, which in turn activates the Rac1 GEFs Tiam and Vav2 to increase the pool of Rac1-GTP (Birukova et al., 2008). Our data showing the barrier-protective nature of Epac1 is concordant with previous studies (Adamson et al., 2008, Baumer et al., 2008, Birukova et al., 2010, Fukuhara et al., 2005). Interestingly, activation of Epac can rapidly restore barrier function and VE-cadherin organization when alcohol is present. Because Epac is expressed in many cell types *in vivo*, a future direction will be to identify and test methods to selectively activate this enzyme in the endothelium as a strategy to ameliorate alcohol-induced microvascular hyperpermeability.

In summary, we report that alcohol intoxication increases microvascular leakage *in vivo*. In addition, our endothelial cell monolayer studies indicate that alcohol significantly alters intercellular junctions, suggesting elevated paracellular transport of fluids and solutes. We also present evidence for involvement of the p38 MAPK and Rac1 in alcohol-induced endothelial barrier dysfunction, and that activation of Epac can rapidly restore barrier integrity in the presence of alcohol. These findings represent an important step in understanding how alcohol impacts overall hemodynamics. Additional studies are necessary to define the cellular and molecular mechanisms by which alcohol impacts the microvascular barrier.

Supplementary Material

Refer to Web version on PubMed Central for supplementary material.

Acknowledgments

Research in this publication was supported by the National Institute on Alcohol Abuse and Alcoholism of the National Institutes of Health under award numbers R21AA020049 and T32AA07577. The content is solely the responsibility of the authors and does not necessarily represent the official views of the National Institutes of Health.

REFERENCES

Adamson RH, Ly JC, Sarai RK, Lenz JF, Altangerel A, Drenckhahn D, Curry FE. Epac/Rap1 pathway regulates microvascular hyperpermeability induced by PAF in rat mesentery. Am J Physiol Heart Circ Physiol. 2008; 294:H1188–1196. [PubMed: 18178724]

Adamson RH, Sarai RK, Clark JF, Altangerel A, Thirkill TL, Curry FE. Attenuation by sphingosine-1-phosphate of rat microvessel acute permeability response to bradykinin is rapidly reversible. Am J Physiol Heart Circ Physiol. 2012; 302:H1929–1935. [PubMed: 22427519]

Baumer Y, Drenckhahn D, Waschke J. cAMP induced Rac 1-mediated cytoskeletal reorganization in microvascular endothelium. Histochem Cell Biol. 2008; 129:765–778. [PubMed: 18392843]

Bilello J, McCray V, Davis J, Jackson L, Danos LA. Acute ethanol intoxication and the trauma patient: hemodynamic pitfalls. World J Surg. 2011; 35:2149–2153. [PubMed: 21748516]

Birukova AA, Burdette D, Moldobaeva N, Xing J, Fu P, Birukov KG. Rac GTPase is a hub for protein kinase A and Epac signaling in endothelial barrier protection by cAMP. Microvasc Res. 2010; 79:128–138. [PubMed: 19962392]

Birukova AA, Zagranichnaya T, Alekseeva E, Bokoch GM, Birukov KG. Epac/Rap and PKA are novel mechanisms of ANP-induced Rac-mediated pulmonary endothelial barrier protection. J Cell Physiol. 2008; 215:715–724. [PubMed: 18064650]

Borbiev T, Birukova A, Liu F, Nurmukhambetova S, Gerthoffer WT, Garcia JG, Verin AD. p38 MAP kinase-dependent regulation of endothelial cell permeability. Am J Physiol Lung Cell Mol Physiol. 2004; 287:L911–918. [PubMed: 15475493]

Breslin JW, Wu MH, Guo M, Reynoso R, Yuan SY. Toll-like receptor 4 contributes to microvascular inflammation and barrier dysfunction in thermal injury. Shock. 2008; 29:349–355. [PubMed: 17704733]

Breslin JW, Yuan SY, Wu MH. VEGF-C alters barrier function of cultured lymphatic endothelial cells through a VEGFR-3-dependent mechanism. Lymphat Res Biol. 2007; 5:105–113. [PubMed: 17935478]

Corada M, Mariotti M, Thurston G, Smith K, Kunkel R, Brockhaus M, Lampugnani MG, Martin-Padura I, Stoppacciaro A, Ruco L, McDonald DM, Ward PA, Dejana E. Vascular endothelial-cadherin is an important determinant of microvascular integrity in vivo. Proc Natl Acad Sci U S A. 1999; 96:9815–9820. [PubMed: 10449777]

Delanoe-Ayari H, Al Kurdi R, Vallade M, Gulino-Debrac D, Riveline D. Membrane and acto-myosin tension promote clustering of adhesion proteins. Proc Natl Acad Sci U S A. 2004a; 101:2229–2234. [PubMed: 14982992]

Delanoe-Ayari H, Lenz P, Brevier J, Weidenhaupt M, Vallade M, Gulino D, Joanny JF, Riveline D. Periodic adhesive fingers between contacting cells. Phys Rev Lett. 2004b; 93:108102. [PubMed: 15447454]

Duran WN, Breslin JW, Sanchez FA. The NO cascade, eNOS location, and microvascular permeability. Cardiovasc Res. 2010; 87:254–261. [PubMed: 20462865]

Duran, WN.; Sanchez, FA.; Breslin, JW. Microcirculatory Exchange Function, in Handbook of Physiology: Microcirculation, Handbook of Physiology: Microcirculation. TUMA, RF.; DURAN, WN.; LEY, K., editors. Academic Press - Elsevier; San Diego, CA.: 2008. p. 81-124.

Edelstein A, Amodaj N, Hoover K, Vale R, Stuurman N. Computer Control of Microscopes Using μManager. Curr Protoc Mol Biol. 2010; 92:14.20.11–14.20.17.

Fabbri A, Marchesini G, Morselli-Labate AM, Rossi F, Cicognani A, Dente M, Iervese T, Ruggeri S, Mengozzi U, Vandelli A. Blood alcohol concentration and management of road trauma patients in the emergency department. J Trauma. 2001; 50:521–528. [PubMed: 11265033]

Fukuhara S, Sakurai A, Sano H, Yamagishi A, Somekawa S, Takakura N, Saito Y, Kangawa K, Mochizuki N. Cyclic AMP potentiates vascular endothelial cadherin-mediated cell-cell contact to enhance endothelial barrier function through an Epac-Rap1 signaling pathway. Mol Cell Biol. 2005; 25:136–146. [PubMed: 15601837]

Garcia JG, Wang P, Schaphorst KL, Becker PM, Borbiev T, Liu F, Birukova A, Jacobs K, Bogatcheva N, Verin AD. Critical involvement of p38 MAP kinase in pertussis toxin-induced cytoskeletal reorganization and lung permeability. FASEB J. 2002; 16:1064–1076. [PubMed: 12087068]

Goldberg PL, MacNaughton DE, Clements RT, Minnear FL, Vincent PA. p38 MAPK activation by TGF-beta1 increases MLC phosphorylation and endothelial monolayer permeability. Am J Physiol Lung Cell Mol Physiol. 2002; 282:L146–154. [PubMed: 11741826]

Greiffenstein P, Mathis KW, Stouwe CV, Molina PE. Alcohol binge before trauma/hemorrhage impairs integrity of host defense mechanisms during recovery. Alcohol Clin Exp Res. 2007; 31:704–715. [PubMed: 17374050]

Haorah J, Floreani NA, Knipe B, Persidsky Y. Stabilization of superoxide dismutase by acetyl-l-carnitine in human brain endothelium during alcohol exposure: novel protective approach. Free Radic Biol Med. 2011; 51:1601–1609. [PubMed: 21782933]

Haorah J, Heilman D, Knipe B, Chrastil J, Leibhart J, Ghorpade A, Miller DW, Persidsky Y. Ethanol-induced activation of myosin light chain kinase leads to dysfunction of tight junctions and blood-brain barrier compromise. Alcohol Clin Exp Res. 2005a; 29:999–1009. [PubMed: 15976526]

Haorah J, Knipe B, Gorantla S, Zheng J, Persidsky Y. Alcohol-induced blood-brain barrier dysfunction is mediated via inositol 1,4,5-triphosphate receptor (IP3R)-gated intracellular calcium release. J Neurochem. 2007; 100:324–336. [PubMed: 17241155]

Haorah J, Knipe B, Leibhart J, Ghorpade A, Persidsky Y. Alcohol-induced oxidative stress in brain endothelial cells causes blood-brain barrier dysfunction. J Leukoc Biol. 2005b; 78:1223–1232. [PubMed: 16204625]

Howard RJ, Slesinger PA, Davies DL, Das J, Trudell JR, Harris RA. Alcohol-binding sites in distinct brain proteins: the quest for atomic level resolution. Alcohol Clin Exp Res. 2011; 35:1561–1573. [PubMed: 21676006]

Jurkovich GJ, Rivara FP, Gurney JG, Seguin D, Fligner CL, Copass M. Effects of alcohol intoxication on the initial assessment of trauma patients. Ann Emerg Med. 1992; 21:704–708. [PubMed: 1590611]

Kevil CG, Oshima T, Alexander JS. The role of p38 MAP kinase in hydrogen peroxide mediated endothelial solute permeability. Endothelium. 2001; 8:107–116. [PubMed: 11572474]

Kiemer AK, Weber NC, Furst R, Bildner N, Kulhanek-Heinze S, Vollmar AM. Inhibition of p38 MAPK activation via induction of MKP-1: atrial natriuretic peptide reduces TNF-alpha-induced actin polymerization and endothelial permeability. Circ Res. 2002; 90:874–881. [PubMed: 11988488]

Kurtz KH, Souza-Smith FM, Moor AN, Breslin JW. Rho kinase enhances contractions of rat mesenteric collecting lymphatics. PloS one. 2014; 9:e94082. [PubMed: 24710574]

Lal BK, Varma S, Pappas PJ, Hobson RW 2nd, Duran WN. VEGF increases permeability of the endothelial cell monolayer by activation of PKB/akt, endothelial nitric-oxide synthase, and MAP kinase pathways. Microvasc Res. 2001; 62:252–262. [PubMed: 11678628]

Lampugnani MG, Corada M, Caveda L, Breviario F, Ayalon O, Geiger B, Dejana E. The molecular organization of endothelial cell to cell junctions: differential association of plakoglobin, beta-catenin, and alpha-catenin with vascular endothelial cadherin (VE-cadherin). J Cell Biol. 1995; 129:203–217. [PubMed: 7698986]

Li SY, Gomelsky M, Duan J, Zhang Z, Gomelsky L, Zhang X, Epstein PN, Ren J. Overexpression of aldehyde dehydrogenase-2 (ALDH2) transgene prevents acetaldehyde-induced cell injury in

human umbilical vein endothelial cells: role of ERK and p38 mitogen-activated protein kinase. J Biol Chem. 2004; 279:11244–11252. [PubMed: 14722101]

Liu F, Schaphorst KL, Verin AD, Jacobs K, Birukova A, Day RM, Bogatcheva N, Bottaro DP, Garcia JG. Hepatocyte growth factor enhances endothelial cell barrier function and cortical cytoskeletal rearrangement: potential role of glycogen synthase kinase-3beta. FASEB J. 2002; 16:950–962. [PubMed: 12087056]

Mathis KW, Molina PE. Transient central cholinergic activation enhances sympathetic nervous system activity but does not improve hemorrhage-induced hypotension in alcohol-intoxicated rodents. Shock. 2009; 32:410–415. [PubMed: 19197225]

Mathis KW, Zambell K, Olubadewo JO, Molina PE. Altered hemodynamic counter-regulation to hemorrhage by acute moderate alcohol intoxication. Shock. 2006; 26:55–61. [PubMed: 16783199]

Mehta D, Malik AB. Signaling mechanisms regulating endothelial permeability. Physiol Rev. 2006; 86:279–367. [PubMed: 16371600]

Molina MF, Whitaker A, Molina PE, McDonough KH. Alcohol does not modulate the augmented acetylcholine-induced vasodilatory response in hemorrhaged rodents. Shock. 2009; 32:601–607. [PubMed: 19197228]

Molina PE, Zambell KL, Norenberg K, Eason J, Phelan H, Zhang P, Stouwe CV, Carnal JW, Porreta C. Consequences of alcohol-induced early dysregulation of responses to trauma/hemorrhage. Alcohol. 2004; 33:217–227. [PubMed: 15596090]

Mountain DJ, Singh M, Menon B, Singh K. Interleukin-1beta increases expression and activity of matrix metalloproteinase-2 in cardiac microvascular endothelial cells: role of PKCalpha/beta1 and MAPKs. Am J Physiol Cell Physiol. 2007; 292:C867–875. [PubMed: 16987994]

Phelan H, Stahls P, Hunt J, Bagby GJ, Molina PE. Impact of alcohol intoxication on hemodynamic, metabolic, and cytokine responses to hemorrhagic shock. J Trauma. 2002; 52:675–682. [PubMed: 11956381]

Reynoso R, Perrin RM, Breslin JW, Daines DA, Watson KD, Watterson DM, Wu MH, Yuan S. A role for long chain myosin light chain kinase (MLCK-210) in microvascular hyperpermeability during severe burns. Shock. 2007; 28:589–595. [PubMed: 17577141]

Shih HC, Hu SC, Yang CC, Ko TJ, Wu JK, Lee CH. Alcohol intoxication increases morbidity in drivers involved in motor vehicle accidents. Am J Emerg Med. 2003; 21:91–94. [PubMed: 12671806]

Souza-Smith FM, Kurtz KM, Molina PE, Breslin JW. Adaptation of mesenteric collecting lymphatic pump function following acute alcohol intoxication. Microcirculation. 2010; 17:514–524. [PubMed: 21040117]

Souza-Smith FM, Molina PE, Breslin JW. Reduced RhoA activity mediates acute alcohol intoxication-induced inhibition of lymphatic myogenic constriction despite increased cytosolic [Ca(2+)]. Microcirculation. 2013; 20:377–384. [PubMed: 23237297]

Spindler V, Schlegel N, Waschke J. Role of GTPases in control of microvascular permeability. Cardiovasc Res. 2010; 87:243–253. [PubMed: 20299335]

Vonghia L, Leggio L, Ferrulli A, Bertini M, Gasbarrini G, Addolorato G. Acute alcohol intoxication. Eur J Intern Med. 2008; 19:561–567. [PubMed: 19046719]

Waschke J, Baumgartner W, Adamson RH, Zeng M, Aktories K, Barth H, Wilde C, Curry FE, Drenckhahn D. Requirement of Rac activity for maintenance of capillary endothelial barrier properties. Am J Physiol Heart Circ Physiol. 2004; 286:H394–401. [PubMed: 14512275]

Waschke J, Burger S, Curry FR, Drenckhahn D, Adamson RH. Activation of Rac-1 and Cdc42 stabilizes the microvascular endothelial barrier. Histochem Cell Biol. 2006; 125:397–406. [PubMed: 16195887]

Yuan SY. Signal transduction pathways in enhanced microvascular permeability. Microcirculation. 2000; 7:395–403. [PubMed: 11142336]

Zhang Y, Zhao S, Gu Y, Lewis DF, Alexander JS, Wang Y. Effects of peroxynitrite and superoxide radicals on endothelial monolayer permeability: potential role of peroxynitrite in preeclampsia. J Soc Gynecol Investig. 2005; 12:586–592.

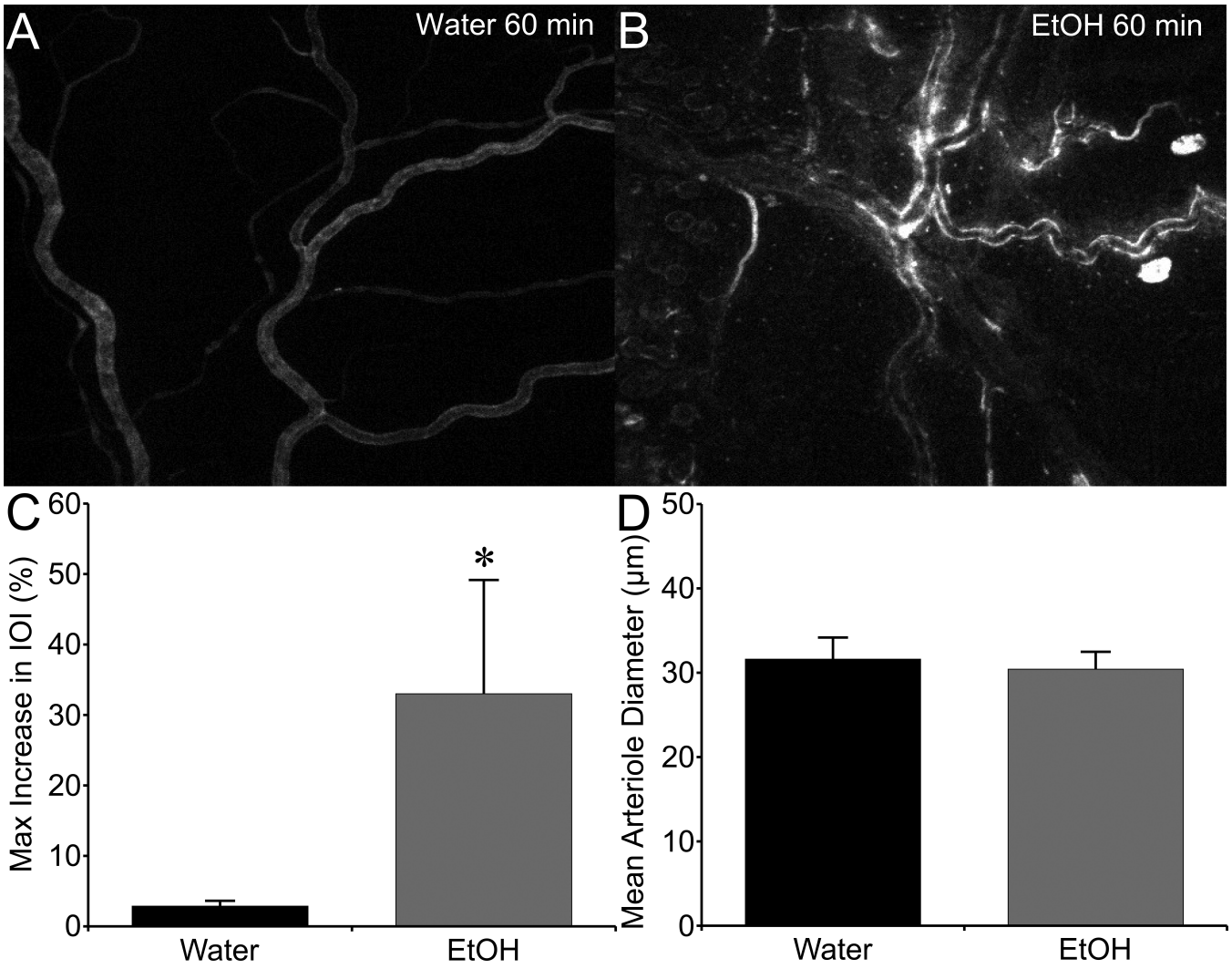

Fig. 1.

Acute alcohol intoxication stimulates microvascular hyperpermeability *in vivo*. *A.* Representative fluorescent image of the mesenteric microcirculation of a control rat that received water, with FITC-albumin present mainly inside the lumens of microvessels. *B.* Representative image of the mesenteric microcirculation from an alcohol-intoxicated rat, in which many leaky sites where FITC-albumin has extravasated into the interstitial space are apparent. *C.* Mean maximum change in IOI in the extravascular space, from the initial baseline just after FITC-albumin was injected i.v. *D.* Mean mesenteric arteriolar diameter in the observed microvascular beds. *P<0.05, alcohol vs. water. N=5 rats studied for the water group, and N=8 rats studied for the alcohol group.

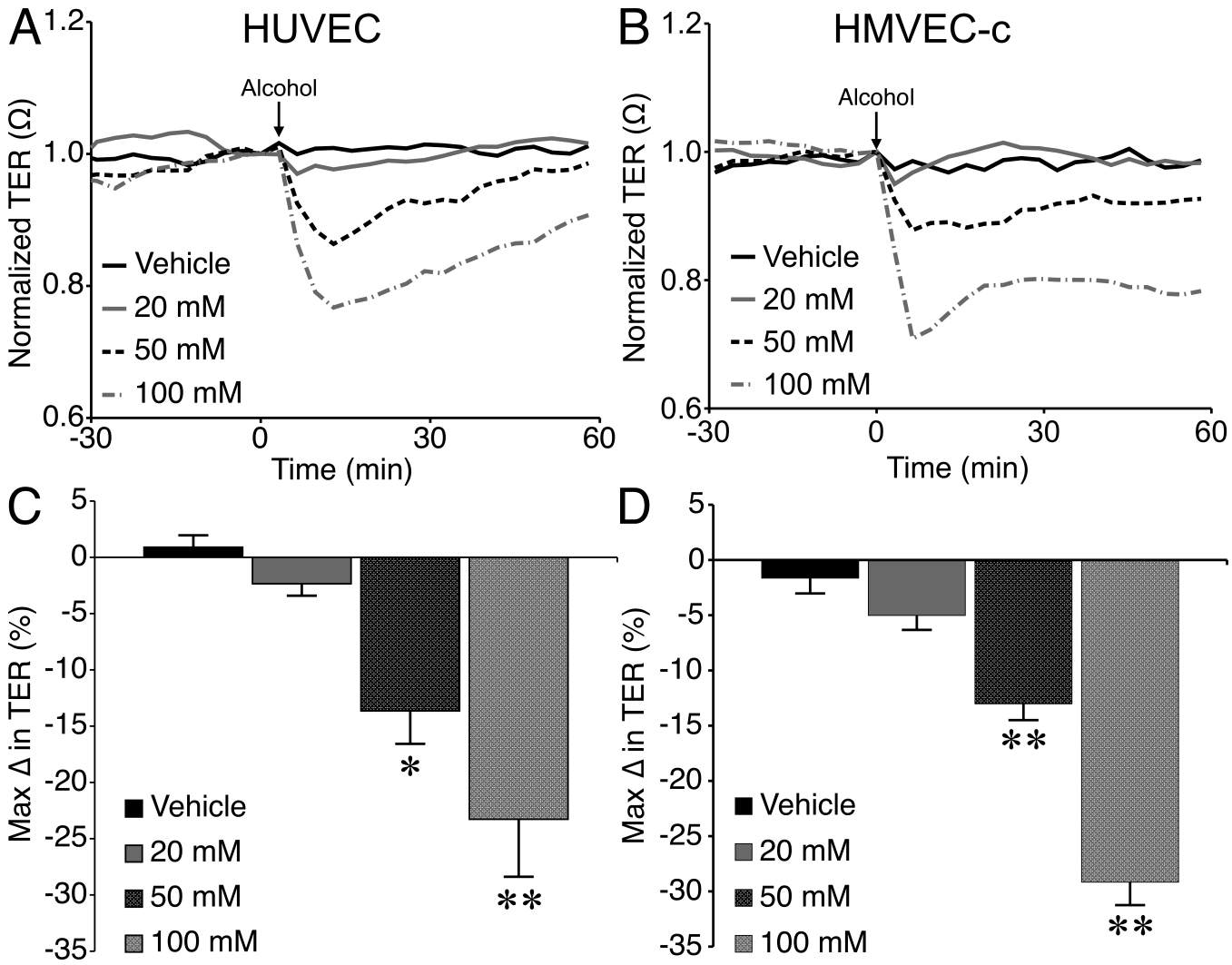

Fig. 2.

Alcohol-induced endothelial barrier dysfunction in cultured endothelial cell monolayers. *A.* Time-course of changes in TER of HUVEC monolayers following application of vehicle (water) or 20, 50, or 100 mM alcohol. *B.* Time course of alcohol-induced changes in TER in HMVEC-c monolayers. *C.* The mean maximum alcohol-induced changes in TER in HUVEC. *D.* Mean maximum alcohol-induced changes in TER in HMVEC-c. *P<0.05 and **P<0.01 vs. vehicle. For all groups, N=4.

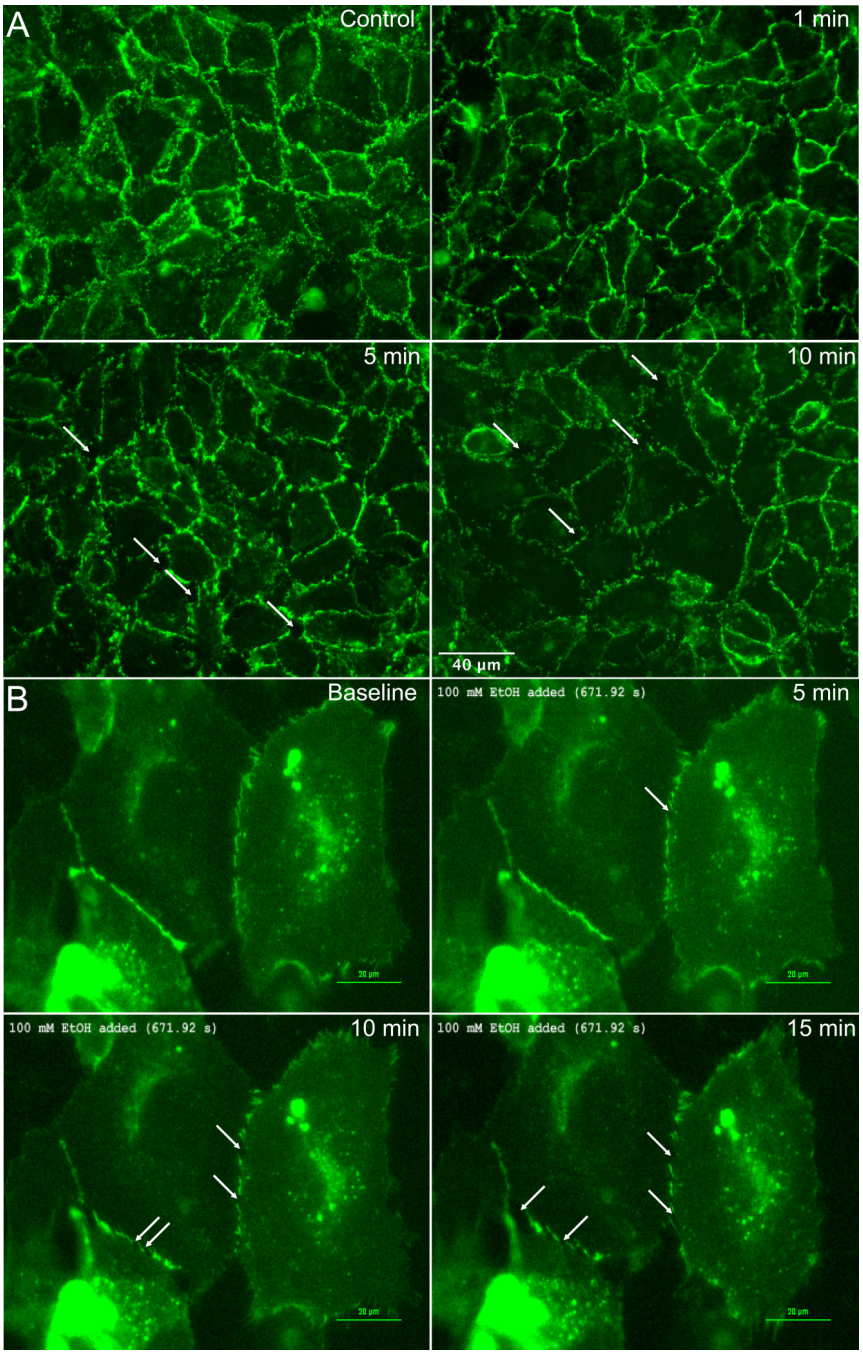

Fig. 3.

Alcohol disrupts VE-cadherin organization at intercellular junctions. *A.* Immunofluorescence microscopy images of VE-cadherin in cultured HUVEC. Cells were either untreated (control) or treated with 100 mM alcohol for 1, 5, or 10 min. *B.* Time-lapse images of VE-cadherin-GFP expressed in HUVEC, before and after treatment with 100 mM alcohol for 5, 10 and 15 min. A confluent monolayer of HUVEC was used for this experiment, but only the HUVEC expressing VE-cadherin-GFP are visible in these time-

lapse images. For both panels *A* and *B*, the images shown are representative of three separate experiments.

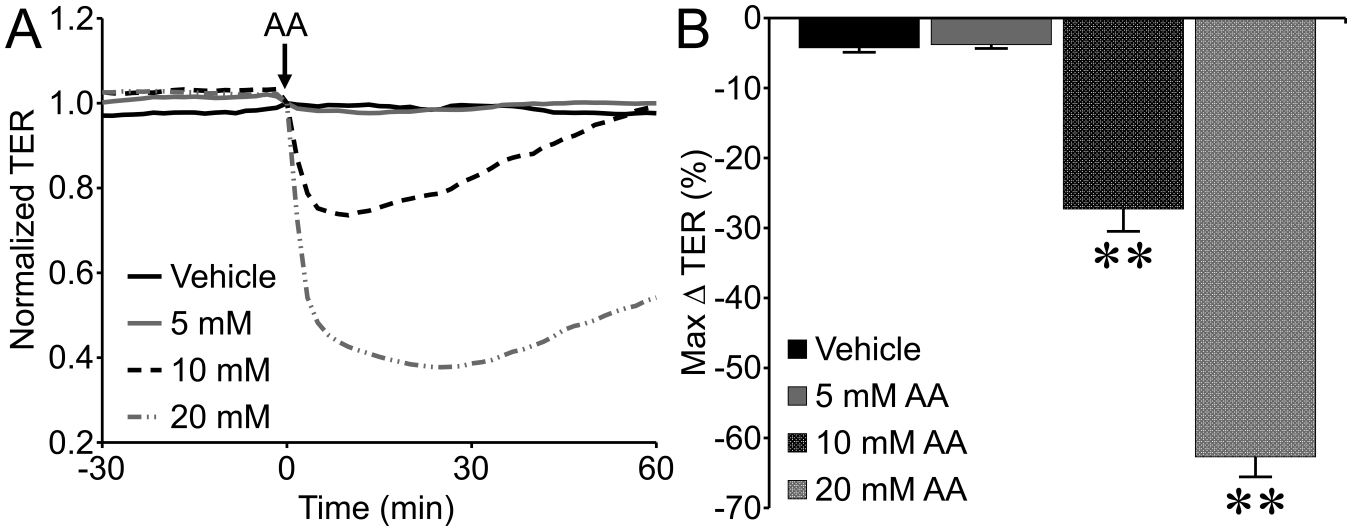

Fig. 4.

Acetaldehyde causes endothelial barrier dysfunction. *A.* Time-course of changes in HUVEC monolayer TER in response to 5, 10, or 20 mM acetaldehyde (AA). *B.* The mean maximum change in TER for each concentration tested. **P<0.01 vs. vehicle (water). For all groups, N=8.

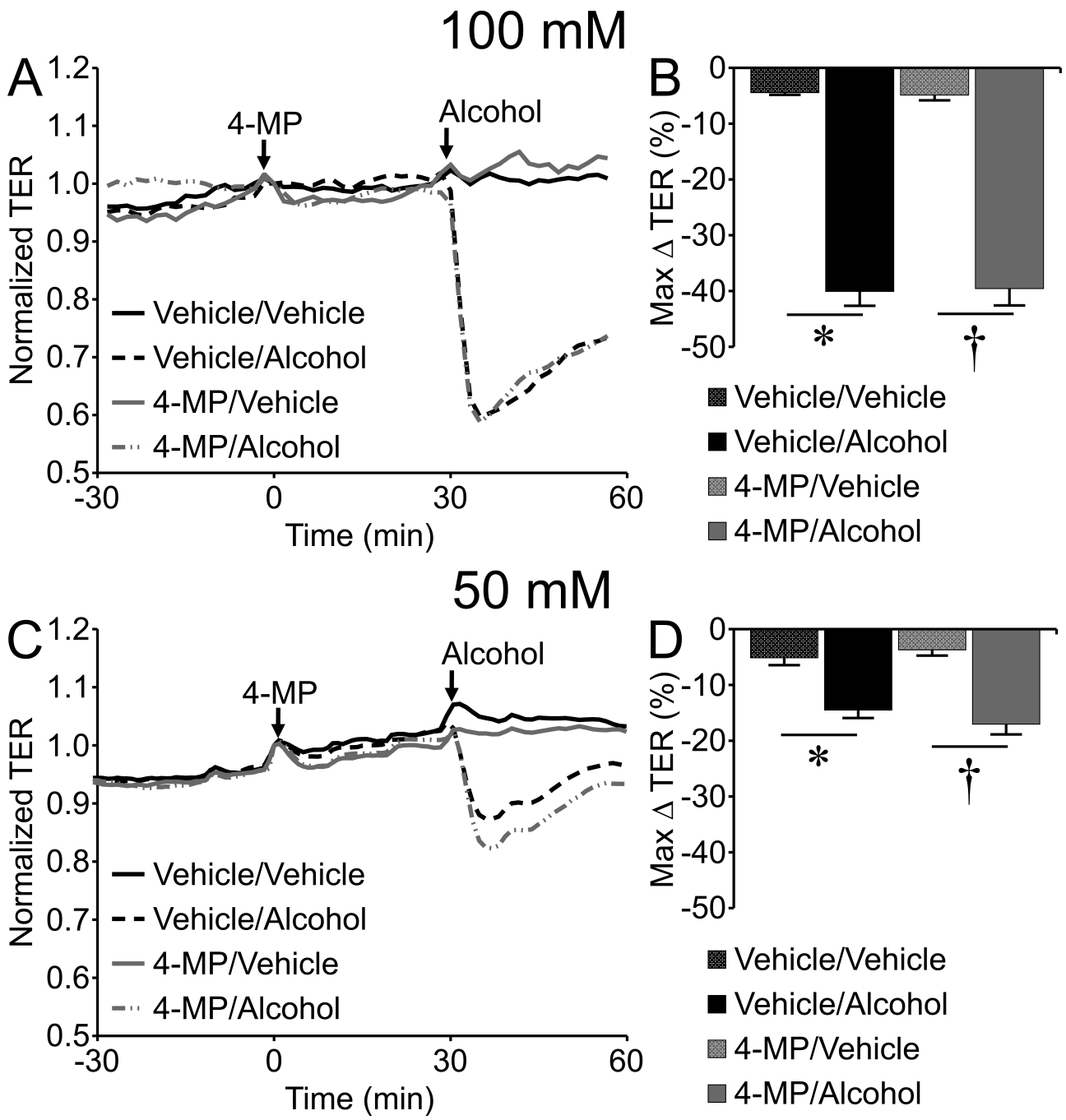

Fig. 5.

Inhibition of ADH with 4-methypyrazole (4-MP) fails to prevent alcohol-induced endothelial barrier dysfunction. (A) Time-course of changes in HUVEC monolayer TER pretreated with 1 mM 4-MP or vehicle (0.17% methanol in water) for 30 min, followed by addition of 100 mM alcohol or vehicle (water). (B) The mean maximum change in TER for each group following and compared to the time point where alcohol was added. (C) Time course with 1 mM 4-MP or vehicle followed by 50 mM or vehicle. (D) Mean maximum

change in TER for each group. *P<0.05 vehicle/alcohol versus vehicle/vehicle, and †P<0.05 4-MP/alcohol versus 4-MP/vehicle. For all treatment groups, N=8.

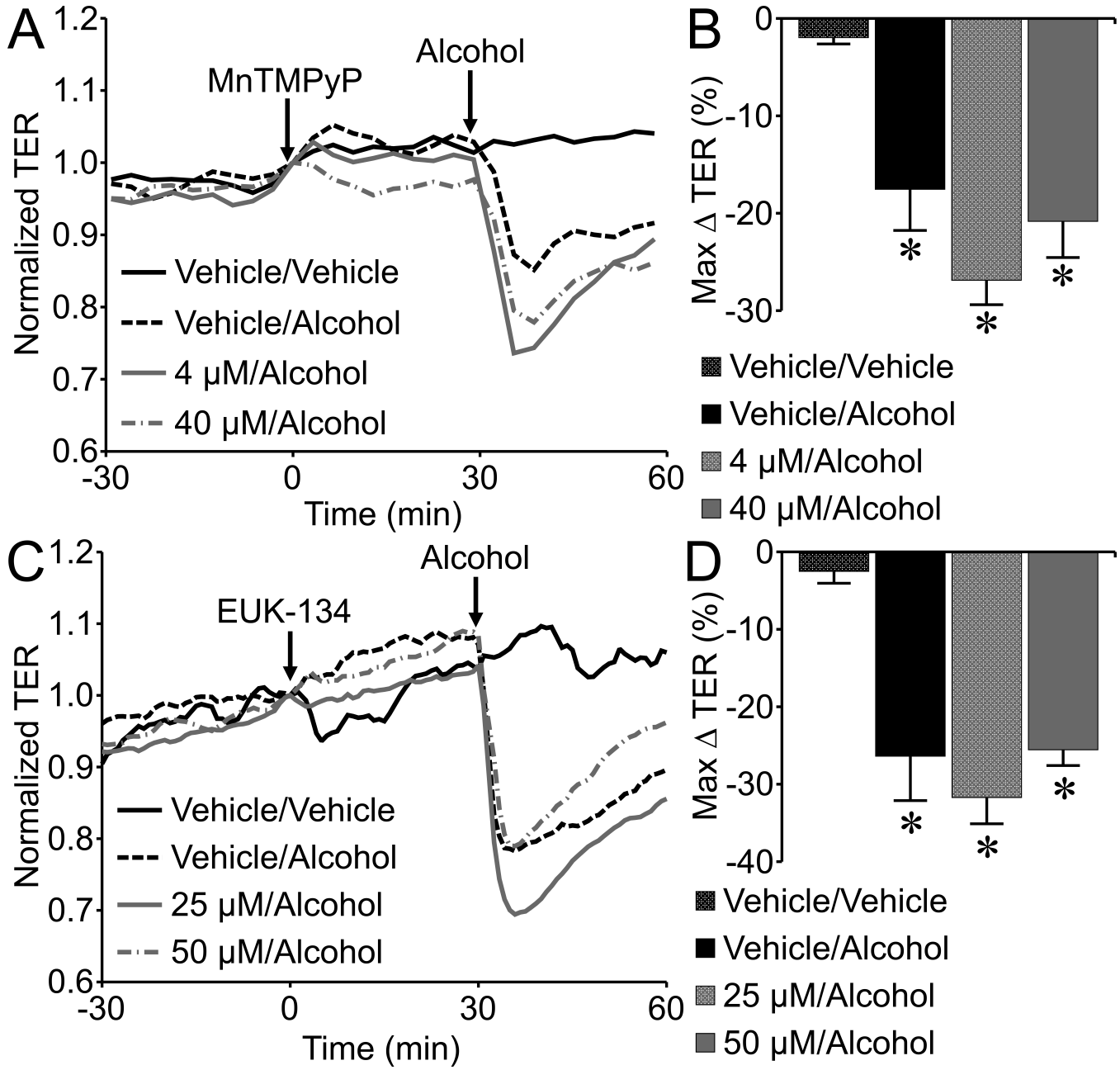

Fig. 6.

The superoxide dismutase mimetic MnTMPyP fails to block alcohol-induced endothelial barrier dysfunction. (A) Time-course changes in TER of HUVEC pretreated with vehicle (water), 4 or 40 μM MnTMPyP for 30 min, followed by 50 mM alcohol. (B) The mean maximum change in TER following 50 mM alcohol in HUVEC treated with vehicle or 4 or 40 μM MnTMPyP. (C) Time-course changes in TER of HUVEC pretreated with vehicle or 25 or 50 μM EUK-134, followed by addition of 50 mM alcohol or vehicle. (D) The mean maximum change in TER following 50 mM alcohol in HUVEC treated with vehicle or EUK-134. *P<0.05 versus vehicle/vehicle group. For all treatment groups, N=4.

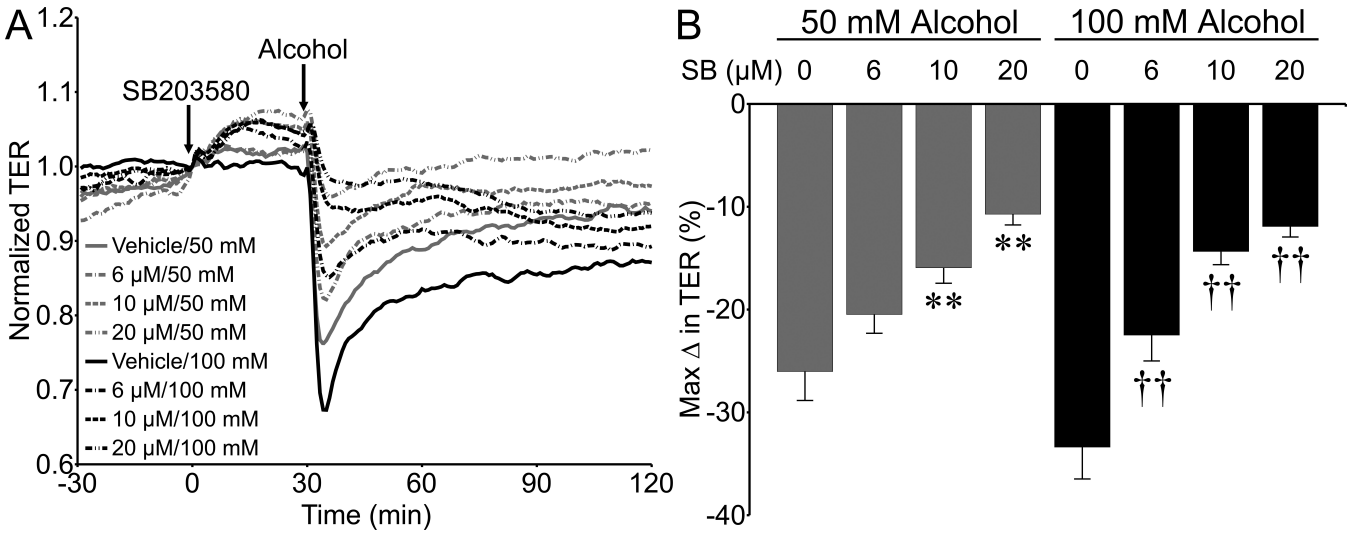

Fig. 7.

Inhibition of p38 MAP kinase significantly attenuates alcohol-induced endothelial barrier dysfunction. A. Time-course changes in TER of HUVEC pretreated with SB203580 or vehicle (0.22% dimethyl sulfoxide in water) for 30 min followed by addition of 50 or 100 mM alcohol or vehicle (water). B. The mean maximum change in TER following and compared to the time point at which alcohol was added. *P<0.0001 vs. vehicle/50 mM alcohol; †P<0.0001 vs. vehicle/100 mM alcohol. For all 50 mM alcohol gropus, N=16. For all 100 mM alcohol groups, N=8.

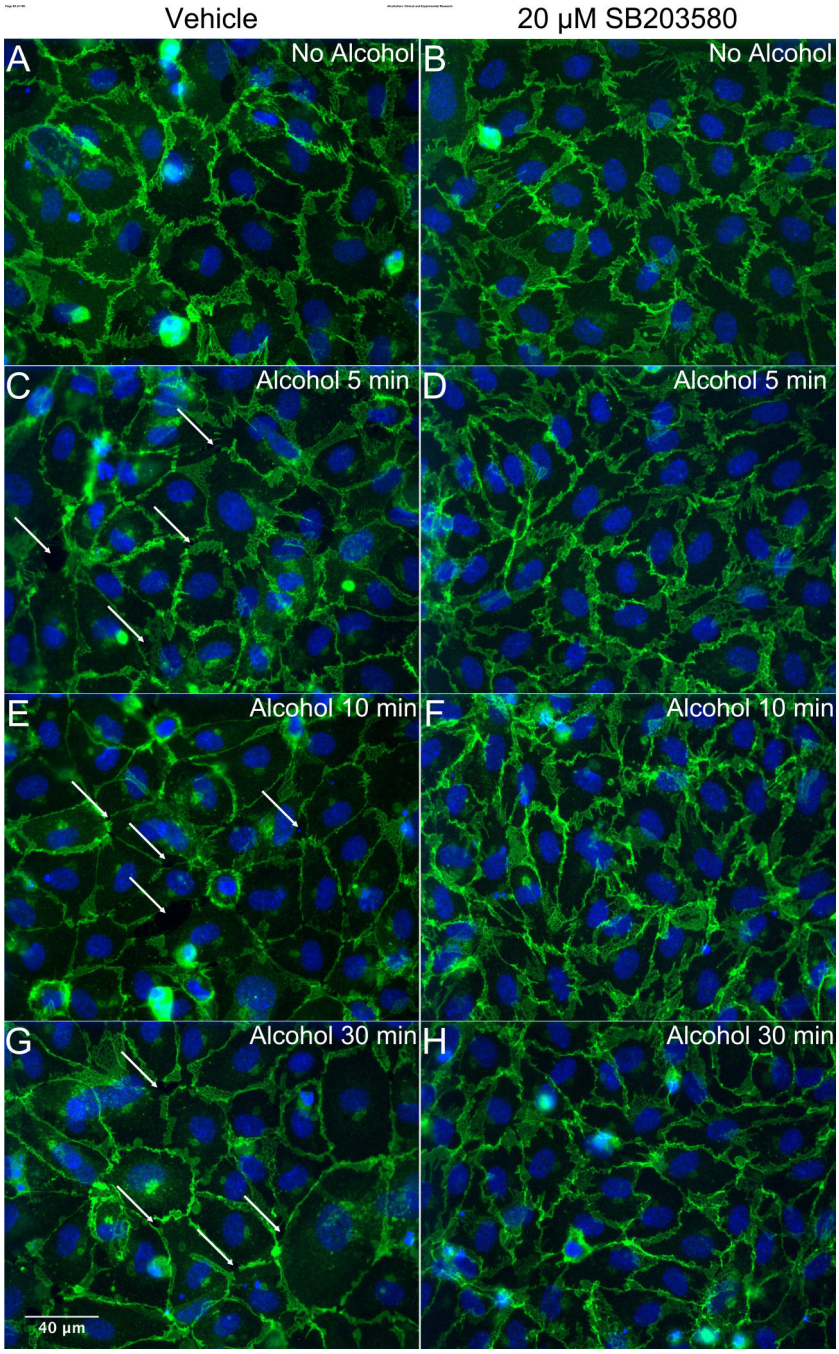

Fig. 8.

Inhibition of p38 MAP kinase blocks alcohol-induced reorganization of VE-cadherin at junctions. Immunofluorescence microscopy images of VE-cadherin in cultured HUVEC are shown. Cells were pretreated with either vehicle (*A*, *C*, *E*, G) or 20 μM SB203580 (*B*, *D*, *F*, H) for 30 minutes followed by 50 mM alcohol for an additional 5, 10, or 30 minutes prior to fixation and labeling. For all panels, the images shown are representative of four separate experiments.

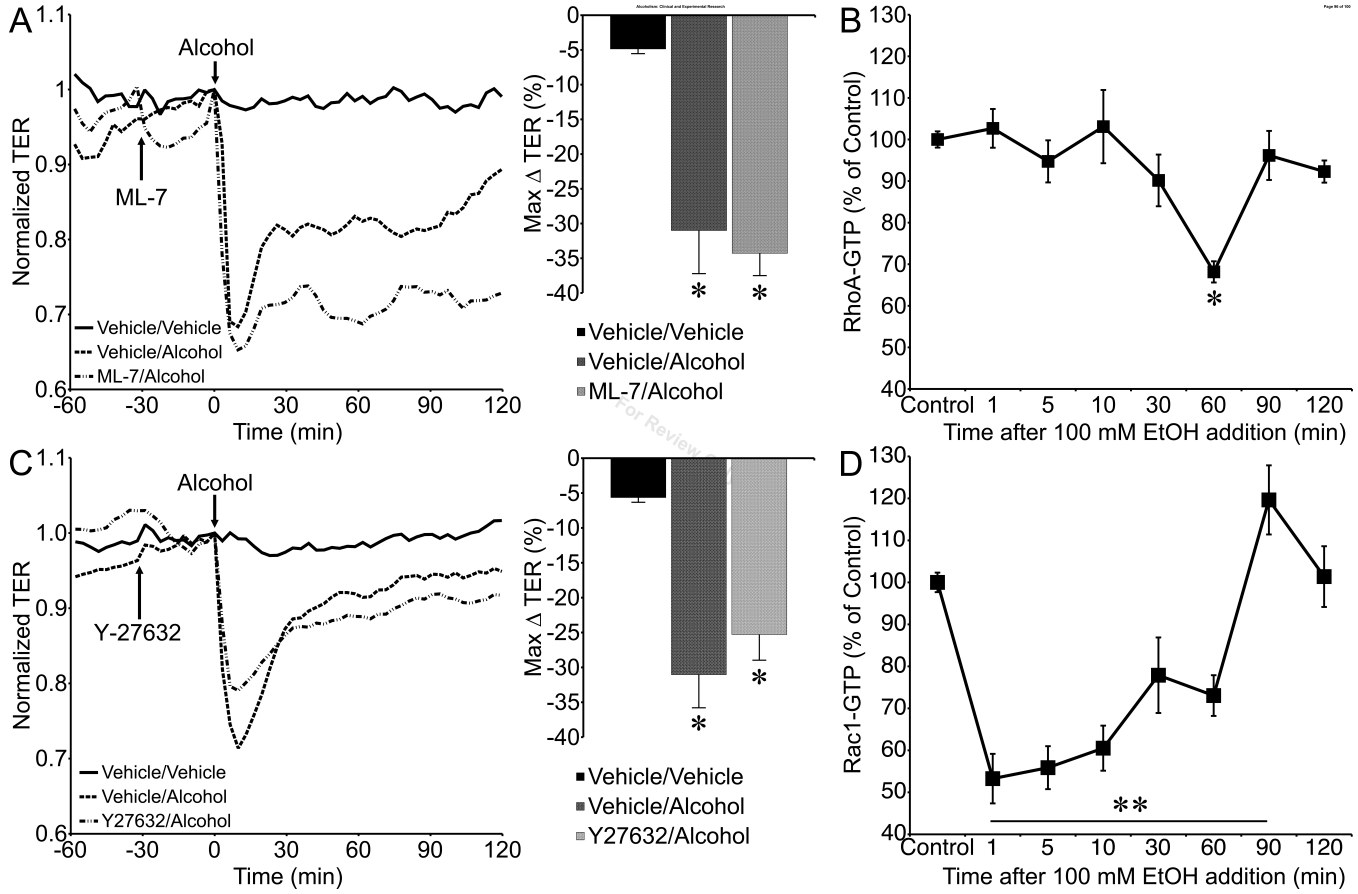

Fig. 9.

Tests of the involvement of MLCK, RhoA/ROCK, and Rac1 in alcohol-induced endothelial barrier dysfunction. *A.* Time-course of the mean changes in TER of HUVEC monolayers pretreated with the MLCK inhibitor ML-7 (1 μM) or vehicle (0.02 % dimethyl sulfoxide in water) prior to 100 mM alcohol, and control HUVEC treated with only both vehicles. The mean maximum changes in TER are also shown in the right hand panel. N=4 for all groups. *B.* Mean RhoA-GTP levels in untreated control cells and those treated with 100 mM alcohol for 1, 5, 10, 30, 60, 90, and 120 min. N=4 for all groups. *C.* Time course of changes in HUVEC monolayer TERs pretreated with 5 μM Y-27632 or vehicle (water) followed by 100 mM alcohol (N=11 each), and vehicle/vehicle control (N=8). The right hand panel summarizes the maximum changes in TER for each group. *D.* Rac1-GTP levels in HUVEC monolayers treated with 100 mM alcohol for 1, 5, 10, 30, 60, 90, and 120 min, and untreated controls. N=4 for all groups. *P<0.05 and **P<0.01 versus control.

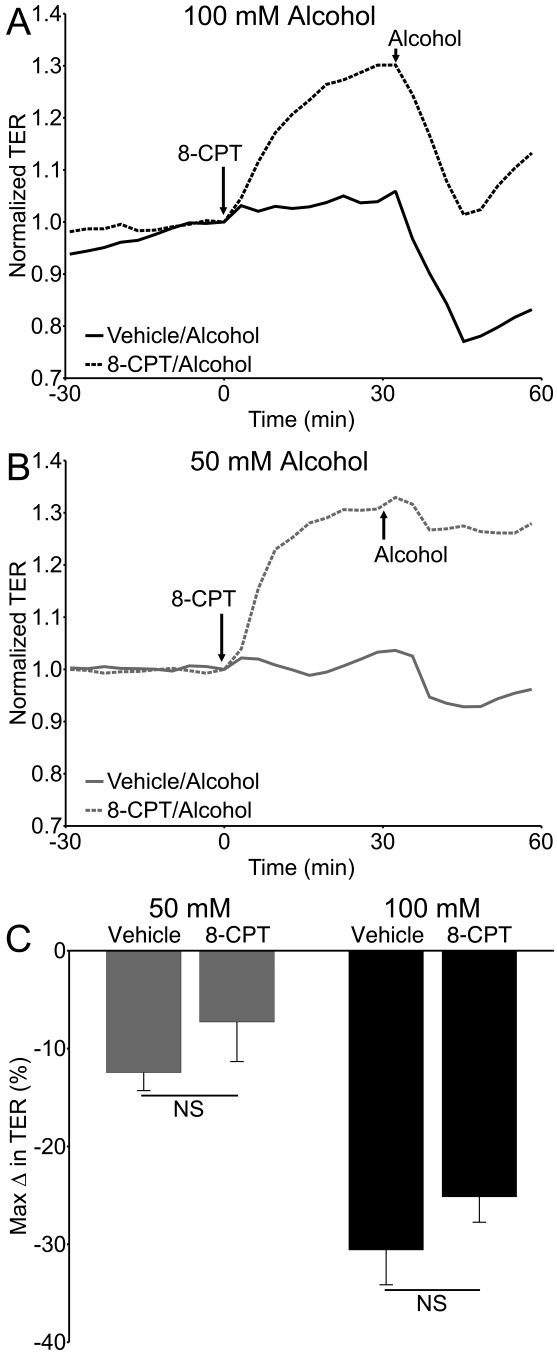

Fig. 10.

Activation of Epac enhances endothelial barrier function, but does not block alcohol-induced decreases in barrier dysfunction. (A and B) Time courses showing changes in TER of HUVEC pretreated with 100 μM 8-CPT or vehicle (water) for 30 minutes followed by addition 50 or 100 mM alcohol. (C) Maximum change in HUVEC TER following addition of alcohol, compared to the time point at which alcohol was added. N=8 for all groups.

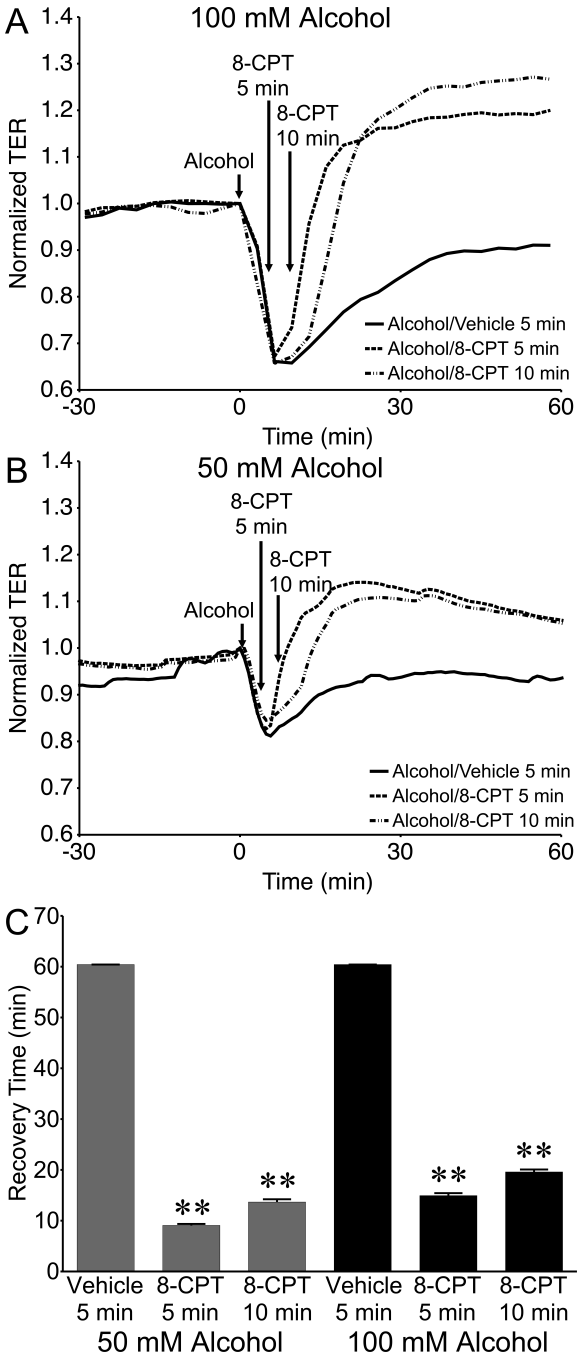

Fig. 11.

Activation of Epac accelerates recovery during alcohol-induced barrier dysfunction. (A and B) Time course of changes in HUVEC monolayer TER in response to 50 or 100 mM alcohol, followed by addition of 100 μM 8-CPT 5 or 10 min later, or vehicle (water) 5 min later. (C) Mean recovery time for HUVEC, i.e. time to return to baseline TER, starting from the time point at which alcohol was added. **P<0.01 versus alcohol/vehicle group. N=12 for all groups.

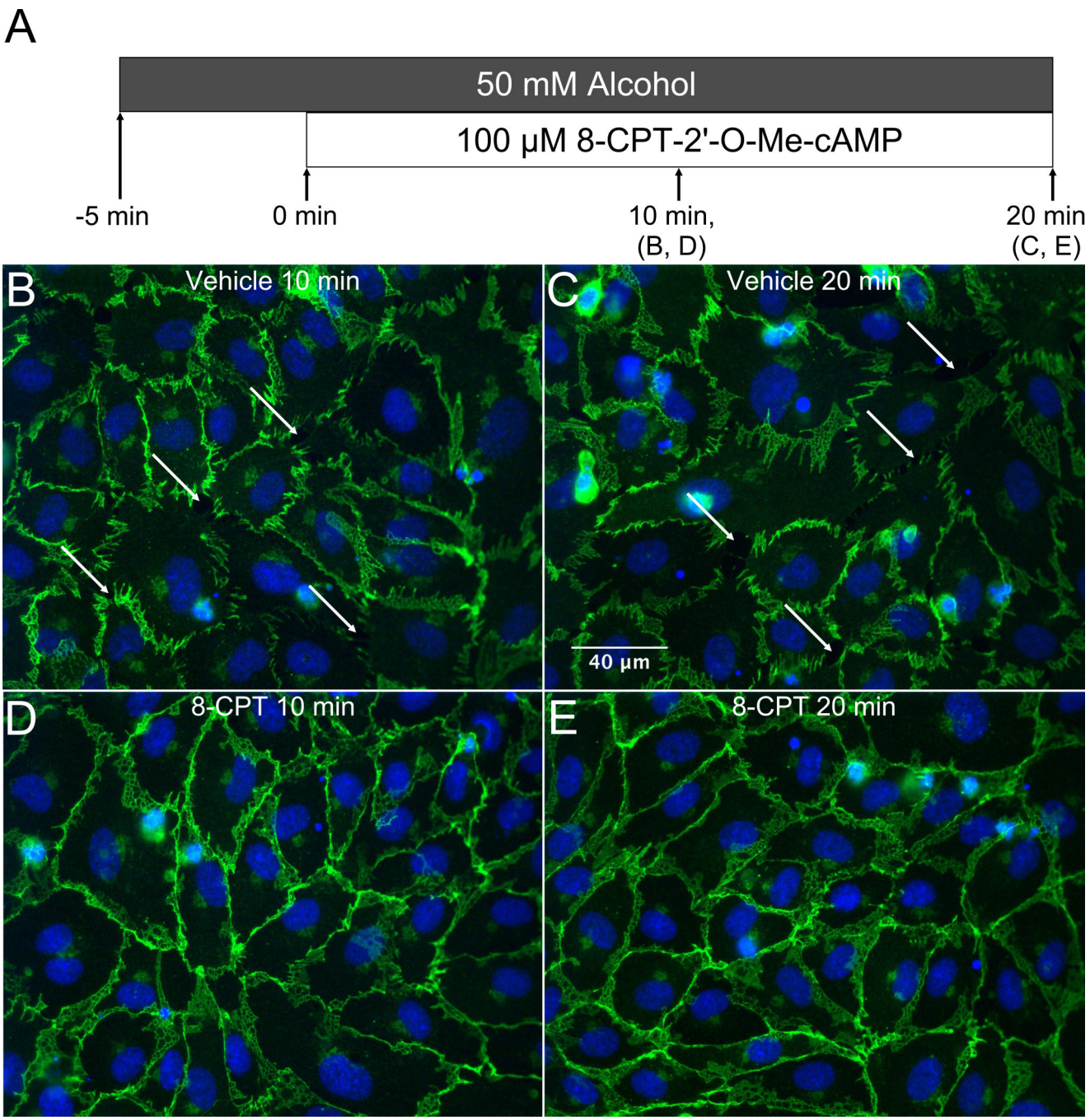

Fig. 12.

Addition of 8-CPT shortly after alcohol treatment inhibits alcohol-mediated reorganization of VE-cadherin. Immunofluorescence microscopy images of VE-cadherin in cultured HUVEC are shown. *A.* Visual representation of experiment timeline. Cells were treated with 50 mM alcohol, and 5 min. later were treated with vehicle (*B,* C) or 100 µM 8-CPT (*D*, *E*). 8-CPT treatment lasted for either 10 or 20 minutes before cells were fixed and labeled. For all panels, images shown are representative of four experiments.